Liquid Crystals
Publication details, including instructions for authors and subscription information:
http://www.informaworld.com/smpp/title~content=t713926090

Photoaligned bistable twisted nematic liquid crystal displays

Martin Stalder[a]; Martin Schadt[a]
[a] Rolic Research Ltd., Gewerbestr. 18, CH-4123 Allschwil, Switzerland,

Online publication date: 11 November 2010

To cite this Article Stalder, Martin and Schadt, Martin(2003) 'Photoaligned bistable twisted nematic liquid crystal displays', Liquid Crystals, 30: 3, 285 — 296
To link to this Article: DOI: 10.1080/0267829031000071275
URL: http://dx.doi.org/10.1080/0267829031000071275

Liquid Crystals, 2003, Vol. 30, No. 3, 285–296

Photoaligned bistable twisted nematic liquid crystal displays

MARTIN STALDER* and MARTIN SCHADT
Rolic Research Ltd., Gewerbestr. 18, CH-4123 Allschwil, Switzerland

(*Received 9 September 2002; accepted 8 November 2002*)

Novel, optically bistable, twisted nematic liquid crystal display configurations obtained using photoaligned and photopatterned substrates are presented. Switching by 360° between two stable twist configurations is shown. Undesired intermediate states which reduce bistability are effectively suppressed by photopatterned domains around picture elements which exhibit different azimuthal- and zenithal-aligning directions. The high degree of stability of the new, domain-stabilized bistable configurations enables the formation of nematic displays with inherent long term optical memory. Display switching at a few volts is demonstrated.

1. Introduction

For various reasons optically bistable nematic liquid crystal displays (LCDs) are meeting with increasing interest. Their optical memory enables images to be displayed without driving voltages being applied, and because re-addressing is only required upon changing the image content, bistable displays consume optimally low power. Moreover, high information content displays based on bistability do not necessarily require the integration of thin film transistors (TFTs) but can be addressed via cost effective passive matrix addressing schemes. For certain applications bistability does not have to be long term, short term memory which extends over the time interval between subsequent refresh signals is sufficient. The degree of bistability of our new photoaligned nematic displays ranges from short to long term and is controlled by the alignment pattern(s).

Except for zenithal bistable nematic displays (ZBD) [1] bistable displays that are based on two twist states with a twist angle difference of 180° [2] and polymer stabilized bistable cholesteric displays [3], most bistable nematic LCDs are based on Berreman's supertwist configurations and variants thereof [4–8]. Supertwisted nematics are also the basis for the photoaligned bistable display configurations presented here.

In the early 1980s Berreman first demonstrated optically bistable super twisted nematic (BTN) configurations [4]. These conventional BTN cells are based on chirally doped nematic films which exhibit different twist configurations between two uniaxially, parallel aligned substrates with parallel bias tilt at the respective boundaries. The three relevant director configurations in such cells are: (1) a ground state Φ_0 with minimal deformation energy and an azimuthal twist angle Φ_0 which is determined by the direction of boundary alignment and chiral dopant concentration; (2) a first metastable state Φ_1 with a twist angle $\Phi_1=\Phi_0-180°$; and (3) a second metastable state Φ_2 with a twist angle $\Phi_2=\Phi_0+180°$. The states Φ_1 and Φ_2 are only temporarily bistable. The deformation energies of these two metastable states are comparable and larger than the energy of the ground state. Uniaxially aligned BTN cells with a 180° twisted ground state Φ_0 exhibit the metastable states $\Phi_1=0°$ and $\Phi_2=360°$.

Electrically switching between metastable twist states depends on the absolute value $|\Phi_i|$ $(i=1,2)$ of the respective twist angles of the two states. Depending on the amount of chiral dopant, the sign of Φ_i can be positive or negative. The low- and the highly-twisted metastable states with their respective twist angles Φ_L and Φ_H are denoted LT and HT.

In a positive dielectric anisotropic nematic director configuration with a BTN ground state, switching of a picture element (pixel) between its metastable twist states occurs via alignment of the LC director parallel to an applied electric field (reset driving pulse), i.e. via an intermediate homeotropic switching state. From this intermediate state, and depending on the shape of the driving pulse, the director relaxes either into the HT or the LT state. However, because the LT and HT states energetically lie above the ground state, both relax back into the ground state upon voltage turn-off. The relaxation time varies from milliseconds to seconds and depends on pixel size. To achieve optical contrast, the LT and HT states must be sufficiently optically different in polarized light. The first BTN cells exhibited very long response times [4]. New interest in BTN displays arose when their response was improved by alternative addressing schemes combined with thinner cell gaps [5].

*Author for correspondence; e-mail: martin.stalder@rolic.ch

Liquid Crystals ISSN 0267-8292 print/ISSN 1366-5855 online © 2003 Taylor & Francis Ltd
http://www.tandf.co.uk/journals
DOI: 10.1080/0267829031000071275

The elastic energy as well as the optical properties of the three states in BTN cells depend on various parameters, such as pretilt and azimuthal angle(s) on the display substrates, cell gap, helical pitch, positioning of polarizers, and LC material parameters. Detailed analyses of the mechanisms behind improved BTN cells were reported by several groups [8–10]. However, uniaxially aligned BTN displays are still hampered by two major drawbacks: (i) by periodic high voltage driving schemes which are required to hold and switch between the two metastable twist states, and (ii) by the insufficient stability of the two metastable switching states.

Berreman suggested three solutions by which to improve bistability [4], namely, to increase the cell gap above 20 μm, to increase the bias tilt angles above a critical angle $\theta = 60^\circ$ and/or to modulate the topology of the display substrates such that the cell gap between pixels becomes significantly smaller than within the pixel area. Unfortunately, these measures either hamper the display response, increase the driving voltage, degrade display contrast and/or require complex manufacturing processes. Alternatively, Hoke and Bos proposed the stabilization of BTN-LCDs using polymer walls to surround the pixels [7]. The walls are generated by exposing the pixels to UV light such that selective photopolymerization and phase separation at the pixel boundaries occurs in the field-on state. The resulting polymer walls suppress the generation of the undesired ground state. Unfortunately, residual photopolymers in the pixel areas tend to degrade display performance when using this interesting approach.

Here we show that the undesired ground state which develops in conventional, uniaxially aligned BTN displays can be effectively suppressed by photopatterning the LC alignment on at least one substrate. As a consequence, nematic supertwist configurations become truly bistable. For alignment patterning to be effective, we show that highly pretilted alignment domains around BTN pixels have to be generated, whereas low pretilt angles are required within the pixels. For the first time, photoalignment has enabled this type of bias tilt patterning.

2. Single substrate domain-stabilized bistable twisted nematic (S1BTN) configurations

Since the degree of stability of photoaligned BTN displays will be shown to depend on specific aligning pattern(s) and because their stability depends on whether only one or both display substrates are patterned, we denote BTN configurations with one domain-stabilized substrate by S1BTN, BTN–LCDs with both substrates photo-patterned will be termed S2BTN.

Figure 1 (*a*) shows a conventional BTN configuration with its two uniaxially aligned substrates and its identical parallel pretilt angles. Figure 1 (*b*) depicts our S1BTN domain-stabilization concept. In both configurations the nematic LC mixture is doped with a chiral additive such that a uniform $\Phi_0 = -180^\circ$ ground state develops. The alignment on the lower substrate of the domain-stabilized S1BTN configuration of figure 1 (*b*) is photo-patterned and exhibits two different bias tilt angles. The bias tilt angle is small within the pixels P and large in the surrounding domains D. The molecular alignment at the upper substrates in the two configurations of figure 1 are identical.

After applying a voltage pulse to a pixel P in either of the two configurations of figure 1, the respective configuration switches into its zero twist state (LT). At the bottom substrates of both configurations, anchoring breaking occurs upon switching (cf. the differently aligned boundary directors in P and D). The voltage-induced generation of the zero twist configuration (LT) within P in the conventional BTN configuration of figure 1 (*a*) leads to a disclination line L around the pixel boundaries. In conventional BTN-LCDs, and due to their uniaxial alignment on both substrates, disclination lines L are repelled from their substrate surfaces and stabilize in the centre of the LC layer [11]. Since the elastic energy of a pixel in its LT state is larger than in the ground state, figure 1 (*a*), the LT configuration within P of a conventional BTN configuration shrinks with time and eventually disappears. This accounts for the insufficient stability of conventional BTN-LCDs.

The domains D around P of our photoaligned and photopatterned S1BTN configuration in figure 1 (*b*) exhibit the same azimuthal alignment direction as the pixels. However, the pretilt is reversed within D and the pretilt angle is much larger than in P, figure 1 (*b*). As a consequence large bias tilt gradients and elastic deformations occur at the pixel boundaries which force the disclination lines L around the pixels of S1BTN configurations to the surface of the lower substrate, figure 1 (*b*). This surface pinning [12], which does not occur in conventional BTN-LCDs, effectively prevents the LT configuration in domain-stabilized BTN configurations from decaying into the elastic ground state. As a consequence, and as shown below, the degree of bistability of the two twist configurations HT and LT is markedly improved in SBTN displays.

3. Realization and properties of S1BTN display configurations

To test the concept of domain stabilization in S1BTN displays with bias tilt patterned substrates, we made cells with a $\Phi_0 = -90^\circ$ ground state. The cells exhibit the two bistable twist states LT ($\Phi_L = +90^\circ$) and HT ($\Phi_H = -270^\circ$) [13]. Cross-sections through the respective

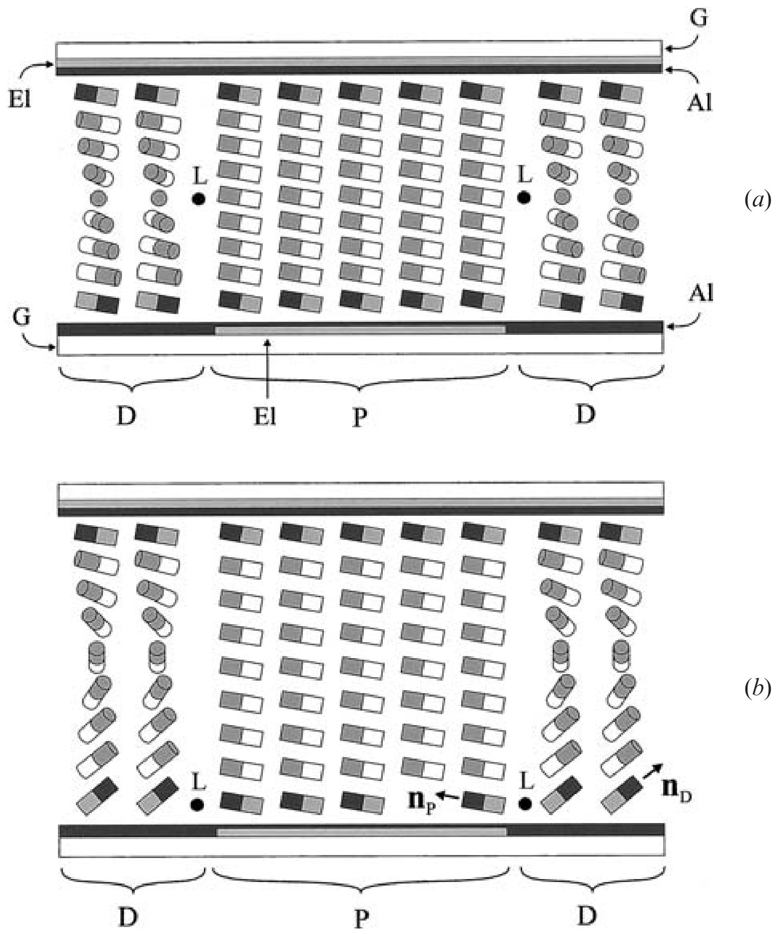

Figure 1. (*a*) Cross-section through a BTN cell with unidirectional alignment layers. The chiral dopant induces −180° twist. After application of an adequate electrical pulse to pixel P, a 0° twist configuration results with a surrounding disclination line L. The 0° twist area is metastable and decays. The upper substrate retains a transparent conductive electrode El, while the bottom electrode El extends only over P. Al = alignment layers, G = glass substrate. (*b*) Cross-section through a S1BTN cell with photoaligned and photopatterned stabilizing alignment domains. The LC directors at the bottom substrate are $\mathbf{n}_P$ (pixel area P) and $\mathbf{n}_D$ (stabilizing domain D). The pixel P is in the bistable 0° state which does not decay into the ground state due to the down-pinned disclination line L.

HT and LT states of a S1BTN stabilized cell are shown in figures 2 (*a*) and 2 (*b*). To achieve the required electrical response and optical contrast, small pretilt angles (2°–15°) are chosen for the pixel areas P, whereas a large pretilt is crucial for D.

Our linear photopolymerization (LPP) technology not only enables the photogeneration of azimuthal aligning patterns but also bias tilt patterns consisting of low- and high-pretilt areas on single substrates [14, 15]. To realize S1BTN-LCDs we used the experimental LPP photopolymer LPP1 from Rolic Research Ltd. to photopattern pretilt domains on one of the substrates of S1BTN cells. P and D domains with different bias tilt angles were generated via a two-step photoexposure through a single photomask [15]. The range of tilt angles which result from LPP1 versus UV exposure time and angle of UV light incidence [15] range from 0° to 70° for the nematic LC mixture 6809 from Merck KGaA. The LC mixture was doped with temperature-compensated chiral dopants from Rolic [16]. The pretilt angle chosen for the top substrate was the same as θ_P in the pixel area P at the bottom substrate.

To achieve sufficiently strong surface pinning of the pixel boundary disclinations in S1BTN LCDs, we found that the pretilt angle θ_D within D must exceed 70°. For a pixel tilt θ_P of 5° this leads to a tilt angle difference between the pretilt in P and D of $\Delta\theta_{PD} = 180° - (\theta_D + \theta_P)$; i.e. less than 105° for the larger pretilt angle difference at the right domain D in figure 1 (*b*). Larger $\Delta\theta_{PD}$ values due to smaller θ_D reduce pinning of the disclination lines and cause the ground state to flow into the pixel area where it destroys bistability. This finding agrees with stability studies made by other groups in non-twisted configurations [12].

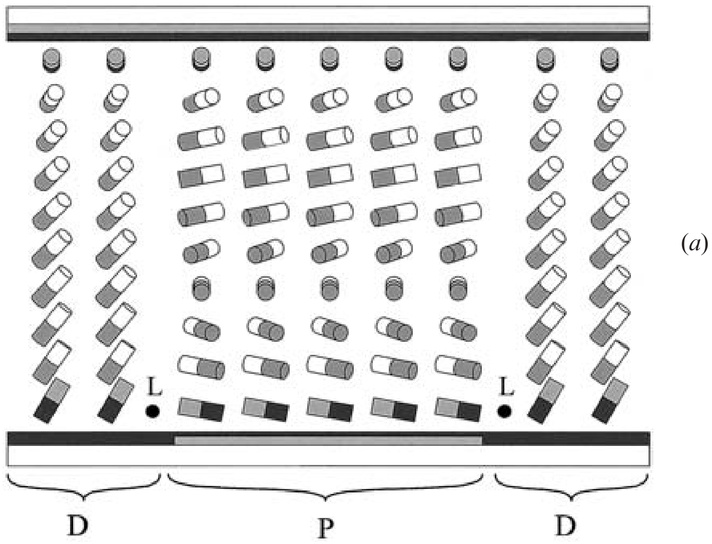

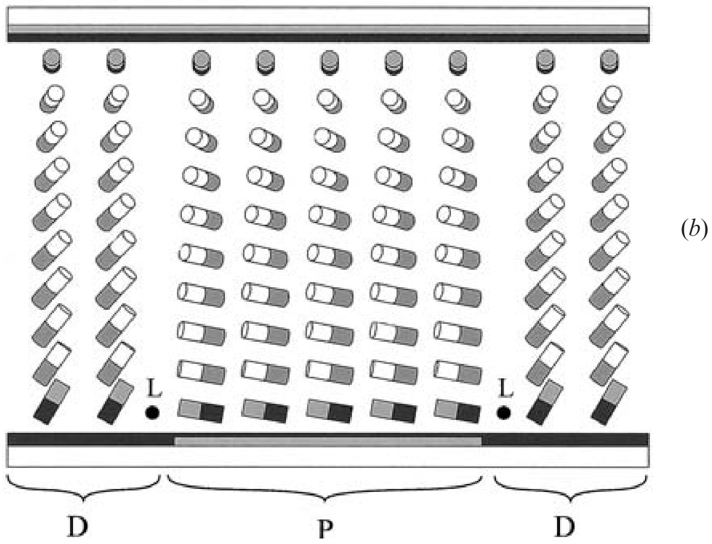

Figure 2. (*a*) Cross-section through a [+90° −270°] S1BTN cell with photoaligned and domain-stabilized alignment. The bistable pixel P is in its bistable −270°C HT state and separated by the stabilizing disclination line L from the ground state domain D (−90°). (*b*) Bistable pixel P in its +90° LT state. The disclination line L is pinned to the bottom alignment layer.

Prototype S1BTN-LCDs were made with $300 \times 300\,\mu m^2$ pixel arrays covering an area of $8 \times 8\,mm^2$. All pixels are addressed in parallel and the cell gap $d = 4.5\,\mu m$. The alignment direction of the pixels is parallel to the pixel borders. After filling, the S1BTN cells are briefly heated to 70°C and 50 V_{rms} is applied for a few seconds, then the cells are rapidly cooled to room temperature under 3 V_{rms} applied. After this treatment the pixels are in one or other of their two bistable states.

Figures 3(*a*) and 3(*b*) show photographs of the two bistable switching states of a photoaligned, domain-stabilized S1BTN-display [+90°, −270°]. The alignment directions of the polarizer, analyser and pixel boundaries are all parallel. In figures 3(*a*) and 3(*b*) the optically non-compensated bistable LT state [+90°] appears green, the disclination lines around the pixels are white, whereas the HT state [−270°] is orange. To switch between the two bistable states, the ratio d/P of the cell gap and the helical pitch P were chosen appropriately. For static stability [+90°, −270°], $d/P = -0.25$ is sufficient; however, under switching conditions, d/P has to be increased [17]. In our case $d/P = -0.37$ was chosen.

4. Stability of S1BTN displays against mechanical stress

An important aspect of bistable displays is their mechanical stability against shock which causes LC flow within the display. To test the shock resistance of our S1BTN-LCDs, the cells were not sealed and spacers were used only at two opposite cell boundaries. Upon exerting pressure on the centre of such a cell, strong LC flow results. Under these shock sensitive boundary conditions the observations made were:

(*a*)

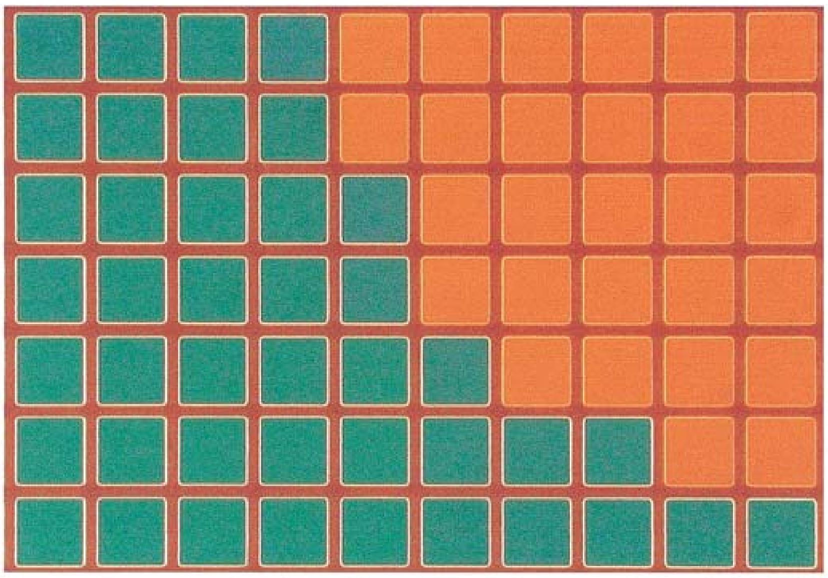

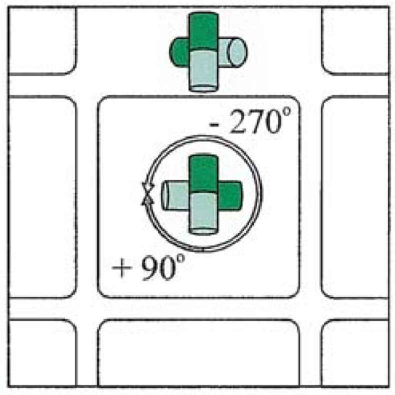

(*b*)

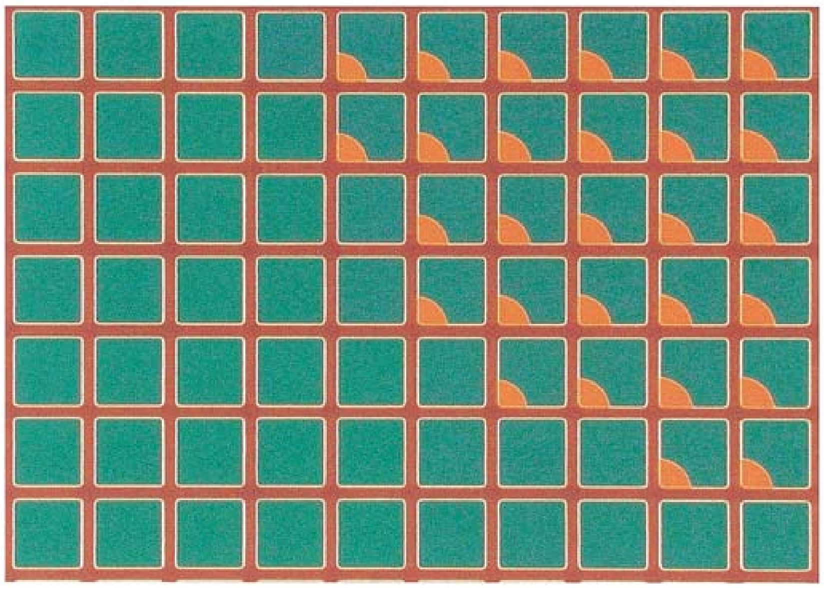

Figure 3. (*a*) Photograph of a [+90° −270°] photopatterned S1BTN-LCD. Green pixels (left) = LT state; orange pixels (right) = HT state. The alignment direction of the display is parallel to the polarizer and analyser. The concentration of chiral additive CM-9209F from Rolic Ltd. is 0.75%; i.e. $d/P = -0.37$. Cell gap 4.5 µm; pixel size 300 µm. (*b*) Photograph of a [+90° −270°] S1BTN-LCD in its LT state after exposure to pressure-induced flow.

(1) The mechanical stability of the HT state against pressure is very good. Even under severe flow—and because the suppressed ground state is stopped by the down-pinned disclination line between pixel P and surrounding domain D—the ground state can virtually not be induced.

(2) Gently squeezing a defect-free pixel in its HT state does not usually cause switching into the LT state. However, short, pulse-type squeezing can lead to a temporary LT state which however decays again upon pressure release.

(3) Exerting flow within a pixel in its LT state causes it to switch into the HT state. This transition usually starts at one of the corners of a square pixel; figure 3(*b*) shows this type of transition. Under these conditions, and once an appreciable

proportion of the pixel area has undergone the transition LT → HT, the entire pixel switches. As will be shown, this type of instability can be remedied with alternative tilt domain configurations.

Around the borders of circularly shaped S1BTN pixels, continuous transitions between all possible adjacent director configurations exist. Therefore, and to identify the critical point around the boundary of an LT pixel where pixel stability is most sensitive to mechanical flow, cells with circularly shaped pixels were made. A picture of a S1BTN-LCD with circular pixels is shown in figure 4 (*a*).

The pixels in figure 4 (*a*) are in their LT state (green). Gently squeezing the cell causes a transition into the HT state (orange) at a boundary point where the difference between two adjacent director configurations is most sensitive to flow. This weakest pixel border position can best be described by the azimuthal angle ψ depicted in figure 4 (*b*). The arbitrary origin $\psi = 0°$ is chosen to coincide with the projection of the pre-tilt direction $-\mathbf{n}_P$ of the pixel; ψ increases counterclockwise. It follows from figure 4 (*a*) that the mechanically most sensitive LT area lies between $\psi = -90°$ and $-180°$, whereas we found very strong flow resistivity (LT stability) to exist between $\psi = 0°$ and $+90°$. This shows that:

(4) The anchoring strength of the LT state at the pixel border strongly depends on the angular position ψ.

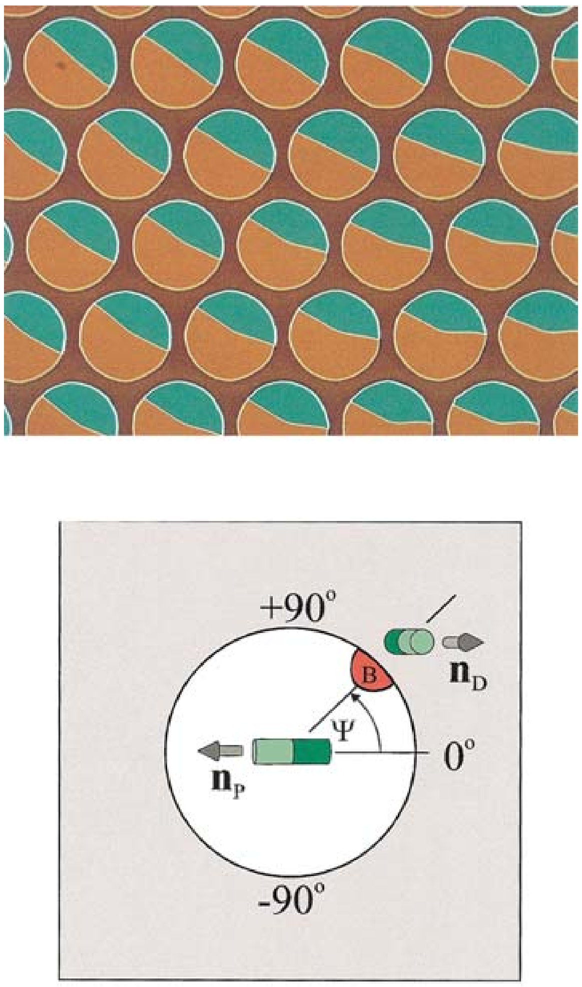

(*a*)

(*b*)

Figure 4. Pixel boundary angle ψ for circularly shaped photo-aligned and domain-stabilized S1BTN pixels (bottom substrate, top view). The mechanically most sensitive LT area lies between $\psi = -90°$ and $-180°$. Strong anchoring exists between $\psi = 0°$ and 90°.

5. Bistable twisted nematic LCDs with dual substrate domain stabilization (S2BTN)

To increase further the bistable anchoring forces in SBTN-LCDs, photoaligned stabilization domains were generated not only on one display substrate, but also on both substrates. The objective was to generate as many as possible of strong LT anchoring sites around each SBTN pixel. To simplify matters, identical alignment patterns were chosen on both substrates which were translated against each other. In an analogous fashion to the S1BTN-LCDs, the aligning patterns on the two substrates of S2BTN-LCDs consist of low pretilt pixel areas and surrounding stabilizing domains with large bias tilt.

The table shows the four possible pixel configurations in [+90°, −270°] S2BTN displays with rectangular shaped pixels which are photoaligned parallel to the pixel boundaries. The table relates different pixel configurations with their respective LT states. Included are the translation directions of the upper substrate with respect to the lower substrate, the associated ψ-values and the domain-induced stability which results from each configuration. Note that the angle ψ on the top substrate increases clockwise and is rotated by 90° with respect to the lower substrate. For comparison, the stability of a single substrate stabilized S1BTN-LCD is included in the table.

Table. Photoaligned and domain-stabilized S1BTN and S2BTN pixels and their stability against a mechanically-induced (LT → HT) transition. LT stability is determined by the weakest boundary position ($-90° \leqslant \psi \leqslant -180°$).

Pixel type	Shift direction	Relevant ψ values	LT stability
S1BTN pixels	n.a.	[0°, 90°, −90°, 180°]	Low
S2BTN pixel A	↗	[0°, 90°]	High
S2BTN pixel B	↘ , ↖	[0°, 90°, −90°, 180°]	Low
S2BTN pixel C	↙	[−90°, 180°]	Low

It follows from the table that three different pixel configurations are possible in S2BTN-LCDs. Pixel configurations B and C exhibit boundaries with $\psi = -90°$ and $-180°$ and are therefore not very stable against mechanical shock, while enhanced LT stability is expected for pixel configuration A with $\psi = 0°$ and 90°. To check the degree of LT stability of the three pixel configurations in the table in one and the same cell, we made S2BTN cells exhibiting a large diagonal shift between the two display substrates, such that all three configurations exist simultaneously. Figure 5 (*a*) depicts arrays of the three S2BTN pixels and figure 5 (*b*) shows four pixels with the relevant ψ values depicted in the schematic on the right. The experiment was started with all pixels in their LT state, figure 5 (*a*) left. When strong mechanical flow is induced, pixels B and C start to undergo a transition into the HT state, where the transition starts at the weakest pixel border location. With increasing LC flow, all weakly anchored pixels eventually decay into their HT state. We found that only the pixel configurations of type A, figure 5 (*a*) right, are strong enough to prevent the LT state from undergoing a transition into the HT state under these severe mechanical stress conditions. The experiment confirms our findings for circular pixels and demonstrates the high degree of bistability which can be achieved with properly photopatterned S2BTN-LCDs.

In a next step S2BTN cells were made consisting of type A pixels only. A section of such a display is shown in figure 5 (*c*). The relative position of the two alignment layer patterns and the corresponding ψ values are depicted on the right. Compared with the simpler pixel geometry of S1BTN-LCDs, photoaligned S2BTN displays comprising only type A domain-stabilized pixels exhibit significantly improved mechanical LT stability. We also found that the width of the high-tilt stabilizing domains can be reduced to a few micrometers without degrading stability.

6. Twist relaxations in photopatterned SBTN displays

Photopatterned and domain-stabilized S2BTN displays are ideal candidates for investigating the slow relaxation phenomena which govern the long term stability of bistable nematic molecular configurations, not only because of the considerably improved bistability of S2BTN displays compared with conventional BTN-LCDs and with S1BTN-LCDs, but also as a result of their design flexibility. With parallel polarizers and LC director alignment parallel to the pixel boundaries, even the minimal changes of pixel interference colours which we found to occur in S2BTN-LCDs over extended periods of time become visible. This spectral sensitivity is barely visible if the pixels are positioned diagonally. We attribute the observed spectral change of interference colours within weeks to be due to very slow twist angle relaxations in BTN configurations.

In S2BTN-LCDs we found in both states (LT and HT) a decrease of twist angles to occur after several weeks. To describe the dynamics of this very slow relaxation qualitatively, the respective initial states which occur immediately after switching are denoted HT* and LT*. After extended periods of time these two initial states relax towards their respective states HT and LT. Estimates of the twist angle differences $\Phi(\mathrm{LT}^*) - \Phi(\mathrm{LT})$ and $\Phi(\mathrm{HT}^*) - \Phi(\mathrm{HT})$ due to twist relaxation are about 6° in 5 μm cells over two months, with the strongest (50%) change occurring within the first 15 min.

A schematic which qualitatively illustrates the twist relaxation mechanism is shown in figure 6. Upon switching the relaxed LT state into the HT* state, the relaxed LC configurations at the alignment boundaries are memorized. This leads to a larger twist angle for the HT* state (see figure 6). The new HT* state relaxes into the HT state. Conversely, if the pixel is switched from HT into the other bistable (LT) state, the LT* state emerges. The reason is analogous to the LT case, i.e. the alignment configuration of the previous HT state is memorized. A similar memory and relaxation effect was reported for weakly anchored 0°–180° nematic wedge cells [18]. Slow relaxation phenomena have not been observed in all our S2BTN-cells. Some domain-stabilized S2BTN cells with 4.5 μm cell gaps essentially maintained their bistability over the entire observation period of more than 16 months.

7. Addressing and optical response of photopatterned and photoaligned SBTN displays

Unlike conventional BTN displays which require reset pulses to break surface anchoring for switching, SBTN displays do not require reset pulses to switch. Simple rectangular bipolar pulses or pulse trains are sufficient to switch between their bistable states [+90°, −270°]. This finding applies to S1BTN- as well as to S2BTN-displays.

The pulse shapes required to switch the S1BTN display of figure 3 is depicted in figure 7 for switching between HT → LT and LT → HT. To switch into HT, typically pulses shorter than 3 ms and voltages larger than 5 V are required. The induced backflow generates the HT state [4]. The minimum pulse length required to switch into the LT state is typically longer than 10 ms for $V < 5$ V. The inset in figure 7 shows the pulse energy required for switching [pulse time × pulse voltage^2]. From figure 7 it follows that the pulse energy for switching is reasonably constant over a broad range of pulse

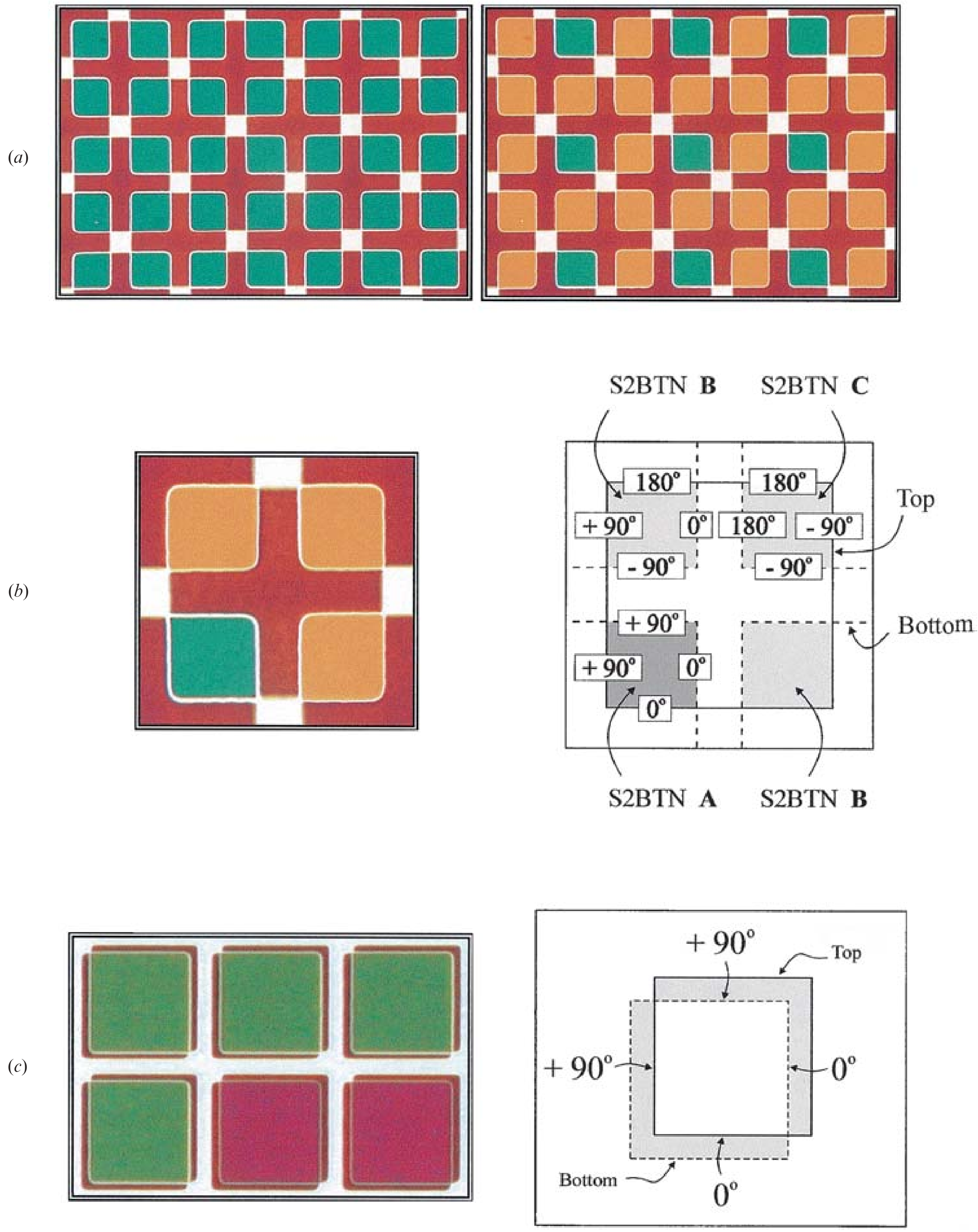

Figure 5. (*a*) Photograph of a S2BTN display with pixels of different LT anchoring strength. The pixels on the left are in their LT state. Only the pixels which are surrounded by strong anchoring borders survive mechanical stress and remain in the LT state, the others switch into the HT state (right). (*b*) Close-up of different pixels (S2BTN A, B and C) and their associated pixel border angle ψ. (*c*) Photograph of a $[+90^\circ \; -270^\circ]$ pixel (type A) of a S2BTN-LCD with two photoaligned and photopatterned substrates. The top picture shows a single pixel surrounded by high tilt domains and the corresponding ψ values. Green pixels = LT state; red pixels = HT state.

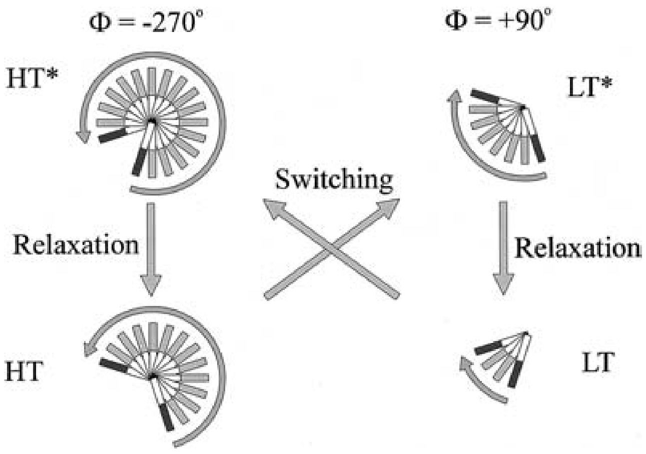

Figure 6. Schematic of twist angle relaxation of the two bistable states in a S1BTN- or S2BTN-LCDs.

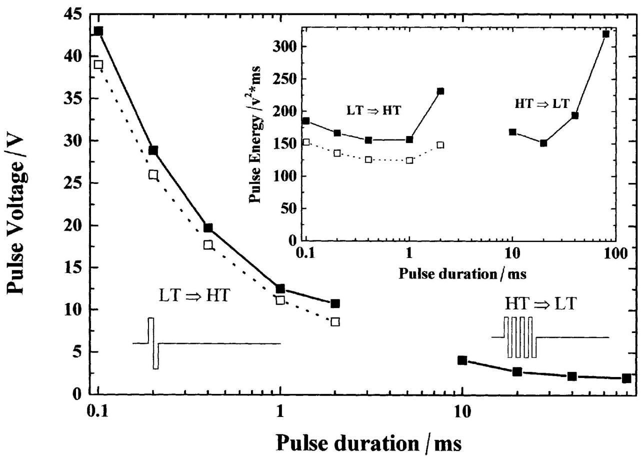

Figure 7. Pulse voltages and durations required to switch a [+90° −270°] S1BTN-LCD with rectangular bipolar pulses or pulse trains.

widths. This agrees with results reported for non-stabilized BTN displays, where reset and selection pulse energy determine switching [19].

The solid line in figure 7 corresponds to saturated switching voltages, resulting in complete switching of the pixels. The dashed line shows the threshold for LT → HT switching, i.e. the voltage at which the first signs of switching become visible. The voltage difference between saturated and threshold switching determines the minimum data voltage required to switch a pixel. According to figure 7, data voltages of at least ±2 V are needed for switching with 100 μs pulses. The HT → LT switching pulses of figure 7 are not optimized; more complex pulse forms and optimized LC materials are expected further to reduce addressing time.

Since the elastic energy of the HT state is lower than that of the LT state, an almost fully switched LT pixel decays within a couple of 100 ms into the HT state, whereas this time reduces to a few ms for a partly switched HT pixel. Since periodically driven passive matrix addressed displays require only temporal bistability, switching from partly switched SBTN pixels is feasible; whereas for display applications requiring long term bistability, LT pixels have to be fully switched.

Figure 8 shows the optical response of an S1BTN display which is driven by the pulses of figure 7. While the optical response for LT → HT switching occurs in less than 50 ms, HT → LT switching is slower and occurs within <200 ms. The LT → HT switching times depend only weakly on the width of the addressing pulses, while the HT → LT switching times depend significantly on pulse length. To reduce further the response times, thinner cell gaps (<2 μm) and/or LC materials with improved viscoelastic properties have to be used.

To matrix address SBTN displays passively, we suggest the addressing scheme depicted in figure 9. The addressing sequence consists of two steps: (i) each pixel is switched into its LT state, (ii) a short selecting pulse in combination with a low voltage data pulse primes the pixel to be switched into the HT state by the row signal. The rows of the display are addressed by an initiating pulse P_L and a short selecting pulse P_S of amplitude V_S. The columns are addressed by data pulses of $\pm V_D$ which are synchronized by the selecting pulses; i.e. the pixels see the difference between row pulses and column data pulses ($V_S \pm V_D$). If a voltage of ($V_S - V_D$) is applied during the selection pulse period, the pixel switches to the LT state. In this case the longer initiating pulse P_L is primarily responsible for switching. For a selection pulse of voltage ($V_S + V_D$) the pixel switches into the HT state. The frequency at which the rows can

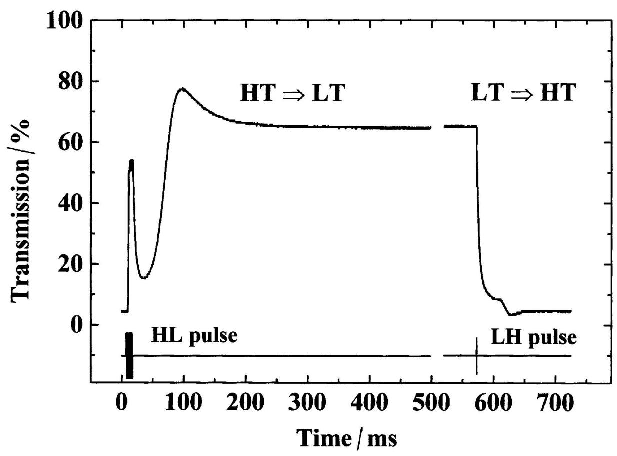

Figure 8. Electro-optical response of an S1BTN-LCD addressed by the pulses shown in figure 7. HT → LT switching is initiated by a pulse train of 20 ms, ±5 V (HL pulse); response time <200 ms. LT → HT switching triggered by a 200 μs pulse of ±28 V (LH pulse); response time <50 ms.

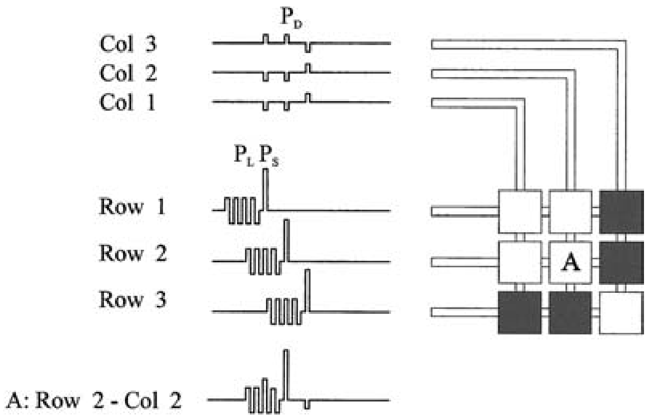

Figure 9. Driving scheme for passive matrix addressing SBTN-LCDs. P_L = initiating pulse, P_S = selecting pulse, P_D = data pulse.

be addressed is primarily determined by the width of the selection pulse. This type of addressing leads to a permanent data background pulse train of $\pm V_D$ which may prevent the display from switching into the HT state. To avoid this problem, the updating rate is reduced which lowers the average background pulse energy and leads to saturated HT switching. There is no upper limit for the number of addressable lines of SBTN-LCDs when using this addressing scheme.

8. SBTN displays performance

To compensate the birefringence colours of our SBTN displays (figure 3) and to achieve black/white images, an optical retarder was placed between the SBTN cell and exit polarizer. As in the above experiments, the 400 pixel configuration of the S1BTN-LCD of figure 3 was used. For near parallel entrance and exit polarizers—with LC cell and retarder in close to diagonal position—a black/white transmission of 60% was achieved at a constrast ratio of 10:1; where 100% transmission is defined as the sum of the photodetector signal for parallel and perpendicular polarizers in the white light of a 100 W halogen lamp. The slow optical axis of the 463 nm retarder is aligned perpendicular to the exit LC director of the pixels. Three switching states of a compensated S1BTN-LCD are shown in figures 10 (*a–e*).

The intermediate display state shown in figure 10 (*b*) is achieved by mechanically squeezing the display which was originally in its white LT state, figure 10 (*a*), such that some pixels are forced into their black HT state. Figure 10 (*e*) shows the black HT state with four white pixels. These white pixels are due to tilt angle defects at the display substrates which prevent the generation of bistable states, i.e. the defective pixels remain in their ground state $\Phi_0 = -90°$ upon switching. For other displays contrast ratios of 20:1 at 75% transmission were measured. Further enhanced brightness and a still larger contrast can be achieved by varying the ground state twist angle Φ_0 and/or the LC layer thickness of the display [10]. However, changing the twist angle Φ_0 of the ground state may also affect the mechanical robustness at the pixel borders. Very recently BTN displays with further improved transmission incorporating one or two optical retarders have been shown [20].

For display applications the temperature dependence of the electro-optical response of S1BTN displays has to be taken into account. Figures 11 (*a*) and 11 (*b*) show the temperature dependence of the addressing signals required for switching S1BTN-LCDs and the corresponding response times.

The pitch of the chirally doped LC mixture is virtually constant over the temperature range 25–70°C. Over this range the display switches reliably into both bistable states. The pulse energy required for LT → HT switching decreases by a factor of four from 25 to 70°C, whereas for HT → LT switching the factor is 2.6. Figure 11 (*b*) shows that the optical response decreases over this temperature range by a factor of three. The electro-optical response times of our early prototype SBTN displays are slower than the 50 ms response times of state of the art STN displays with optimal LC mixtures and cell gaps [21].

9. Conclusions

The degree of stability of bistable twisted nematic (BTN) displays is shown to improve considerably in nematic twist configurations generated by photoaligned and domain-stabilized bias tilt angle patterns on one or both display substrates. High pretilt domains around low pretilt pixels in domain-stabilized (SBTN)-LCDs are shown to cause strong surface pinning of the director dislocation lines, thus markedly improving bistability. The dimensions of the stabilizing alignment domains can be made as small as a few micrometers. Stabilizing domains have become feasible with the emergence of the LPP photoalignment technology and novel LPP photopolymer materials.

BTN display configurations with tunable robustness against mechanical shock are presented. Bistable twisted nematic displays comprising two photoaligned substrates with domain-stabilized bias tilt patterns (S2BTN-LCDs) are shown to exhibit excellent robustness against relaxation of the critical low twist state into the high twist state, i.e. the LT → HT transition. By spacing the display, not only at its boundaries but also within the display area, LC flow is reduced and the degree of bistability of S2BTN-LCDs is expected to meet the most stringent stability requirements. In constrast to ferroelectric displays, SBTN displays are self-healing. If a LT

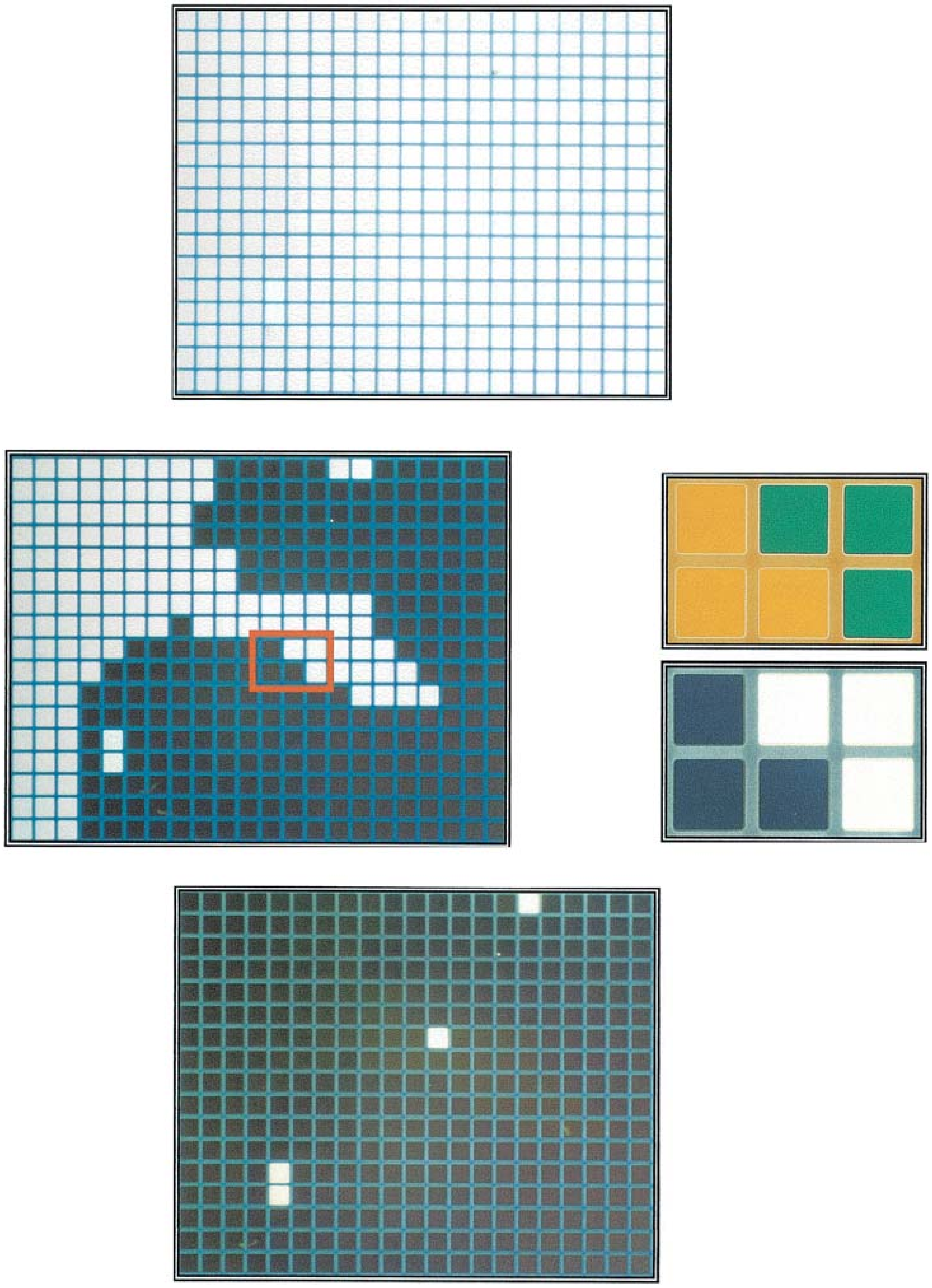

Figure 10. (*a*–*e*) Photograph of the pixel array of the [+90° −270°] S1BTN-LCD of figure 3 incorporating an optical retarder film (463 nm) to achieve black/white response. (*b*) Partly switched pixel array. White pixels: LT state (*a*); black pixels; HT state (*e*). Six enlarged pixels without retarder (*c*) and with retarder (*d*).

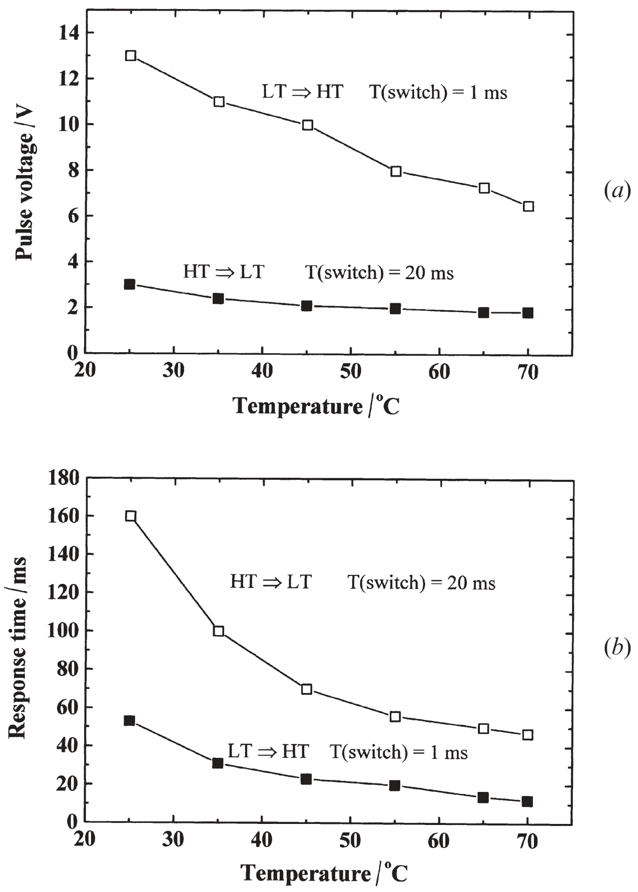

Figure 11. Pulse voltages (*a*) and response times (*b*) of a S1BTN-LCD versus temperature for both switching directions.

pixel should undergo a flow-induced transition into the HT state, the pixel can be switched-back without detrimental optical consequences.

Incorporation of uniaxial optical retarder(s) into SBTN-LCDs is shown to result in black/white display operation. Our photoaligned SBTN-LCDs are at an early prototype stage. Further efforts are required to achieve shorter response times, lower operating voltages and, last but not least, simpler domain patterns suitable for mass production.

The authors thank T. Schacher for the careful sample preparation and J. Fünfschilling and H. Seiberle for valuable discussions.

References

[1] Jones, J. C., Wood, E. L., Bryan-Brown, G. P., and Hui, V. C., 1998, *SID 98 Dig.*, 858.
[2] Dozov, I., and Durand, G., 1998, *Liq. Cryst. Today*, **8,** 1.
[3] Yang, D. K., Huang, X. Y., and Zhu, Y. M., 1997, *Annu. Rev. Mater. Sci.*, **27,** 117.
[4] Berreman, D. W., and Heffner, W. R., 1981, *J. appl. Phys.*, **52,** 3032.
[5] Tanaka, T., Sato, Y., Inoue, A., Momose, Y., Nomura, H., and Iino, S., 1995, *IDRC Asia Display 1995*, 259.
[6] Qian, T. Z., Xie, Z. L., Kwok, H. S., and Shen, P., 1997, *Appl. Phys. Lett.*, **71,** 596.
[7] Hoke, C. D., and Bos, P. J., 1998, *SID 98 Dig.*, 854.
[8] Lee, G. D., Park, K. H., Jang, K. C., Yoon, T. H., Kim, J. C., and Lee, E. S., 1999, *Jpn. J. appl. Phys.*, **38,** 809.
[9] Berreman, D. W., 1983, *Phil. Trans. R. Soc. Lond.*, **A309,** 203.
[10] Yeung, S., Kwok, S. K., Fok, B., Lam, B., Chang, C., and Tsoi, I., 1999, *IDW'99*, 301.
[11] De Gennes, P. G., and Prost, J., 1995, *The Physics of Liquid Crystals* (Oxford: Clarindon Press).
[12] Cheng, J., 1981, *J. appl. Phys.*, **52,** 724.
[13] Xie, Z. L., and Kwok, H. S., 1998, *J. appl. Phys.*, **84,** 77.
[14] Schadt, M., Schmitt, K., Kozinkov, V., and Chigrinov, V., 1992, *Jpn. J. appl. Phys.*, **31,** 2155.
[15] Schadt, M., Seiberle, H., and Schuster, A., 1996, *Nature*, **381,** 212.
[16] Schadt, M., and Fünfschilling, J., 1990, *Jpn. J. appl. Phys.*, **29,** 1974.
[17] Wang, B., and Bos, P. J., 2001, *Jpn. J. appl. Phys.*, **90,** 552.
[18] Sato, Y., Sato, K., and Uchida, T., 1992, *Jpn. J. appl. Phys.*, **31,** L579.
[19] Oh, J. S., Pang, S. C., Lee, H. Y., Yoo, J. G., Kang, K. H., and Lee, E. S., 1999, *IDW'99*, 269.
[20] Guo, J.-X., and Sun, X. W., 2002, *Jpn. J. appl. Phys.*, **41,** 2046.
[21] Blinov, L. M., and Chigrinov, V. G., 1994, *Electrooptic Effects in Liquid Crystal Materials* (New York: Springer Verlag).